Optimal Re-Entry Maneuvers with Bounded Lift Control

L. Beiner *
Tel Aviv University, Ramat Aviv, Israel

Green's theorem is employed to find the optimal lift control that transfers a hypervelocity vehicle between prescribed initial and final values of the altitude and flight-path angle when maximum lift coefficient is bounded. Payoffs to be extremized are either final velocity, range, time, or heat input. Problem formulation leads to linear control, and the optimal maneuvers consist of either max-lift/min-lift or min-lift/max-lift nonsingular paths. Conditions for the final state to be reachable by such sequences are derived. Only descending or ascending trajectories are considered. Analytical solutions are derived, and order of subarcs and locations of switching points are determined. Results of parametric studies in nondimensional form are presented graphically.

Nomenclature

a = constant, Eq. (31)
C = integration constant, Eq. (30)
C_D = drag coefficient
C_{D_0} = zero-lift drag coefficient
C_D^* = drag coefficient at $(L/D)_{max}$
C_L = lift coefficient
C_L^* = lift coefficient at $(L/D)_{max}$
C_F' = equivalent skin-friction coefficient
D = drag force
E^* = $(L/D)_{max}$
g = acceleration of gravity
K = induced drag factor
L = lift force
m = vehicle mass
Q = convective heat input
q = nondimensional convective heat input
r = distance from center of Earth to vehicle
S = aerodynamical reference area
s = nondimensional independent variable
t = time
V = velocity
v = nondimensional velocity
X = range
x = nondimensional range
Z = altitude
z = nondimensional altitude
β = atmosphere scale height
γ = flight-path angle, positive below horizon
λ = normalized lift coefficient
ρ = atmospheric density
ρ_0 = reference density value

Subscripts

I = initial point
F = final point
C, D = switching points

Introduction

ANALYTICAL solutions to the problem of optimal maneuvering of a hypervelocity glider can be obtained by using the Allen and Eggers approximation,[1] which states that, during a skip maneuver, aerodynamic forces are much larger than gravitational so that centrifugal and hence gravitational forces can be neglected. This assumption was first introduced to analyze optimal trajectories in Ref. 2, and various extensions in two and three dimensions were made in Refs. 3–9 (see the excellent monograph by Vinh[10] for a thorough review). Other assumptions included in deriving the solutions were parabolic drag polar, exponential atmosphere, and constant gravitational acceleration. Such analytical solutions employed in their range of validity are useful to verify numerical algorithms, allow insight into the structure of the optimal control, and permit rapid comparative analyses of different maneuvers.

Optimal skip maneuvers in the vertical plane with an upper bound imposed on the magnitude of the lift coefficient have been analyzed in detail in Ref. 4 using optimal control theory; the results show that optimal paths generally involve bounded lift arcs, as well as arcs flown with variable lift, and also that determining the variable lift control and the location of switching points requires, in general, the integration of an equation of motion and/or the solution of a set of nonlinear algebraic equations. However, an extremely simple solution to the same problem based on Green's theorem[11] can be developed for the particular case in which the optimal trajectory involves *only* maximum positive and negative lift arcs. The basic idea of such a solution has been formulated in a simplified context in Ref. 12, but no numerical applications were attempted. The present paper extends and generalizes this approach in order to solve the problem of transferring a hypervelocity glider between prescribed initial and final altitudes and flight-path angles with bounded lift control. Using the concept of region of admissible paths, it is shown that trajectories consisting of a max-lift/min-lift or min-lift/max-lift sequence can extremize either the final velocity, the range, the time, or the heat input. Conditions that permit the final state to be reachable by such sequences are developed, closed-form solutions are derived, and results of parametric studies are presented. The present approach allows one to visualize and to determine simply the existence and nature of the extremum, the number of subarcs, their sequence, and the location of switching points.

Equations of Motion and Constant Lift Solutions

The two-dimensional equations of motion of a point mass vehicle flying in the stationary atmosphere of a spherical

Received Jan. 9, 1986; revision received June 3, 1986.

*Adjunct Associate Professor, Department of Solid Mechanics, Materials and Structures, Faculty of Engineering.

nonrotating Earth are

$$\dot{X} = V\cos\gamma \tag{1}$$

$$\dot{Z} = -V\sin\gamma \tag{2}$$

$$m\dot{V} = -D + mg\sin\gamma \tag{3}$$

$$-mV\dot{\gamma} = L - m\left[g - \left(V^2/r\right)\right]\cos\gamma \tag{4}$$

where γ is positive below the horizon and the lift and drag forces are given as

$$\begin{bmatrix} L \\ D \end{bmatrix} = \tfrac{1}{2}\rho SV^2 \begin{bmatrix} C_L \\ C_D \end{bmatrix} \tag{5}$$

The time rate of change of total convective heat input is given by the following law:[13]

$$\dot{Q} = \tfrac{1}{4}SC_F'\rho V^3 \tag{6}$$

where C_F' is assumed constant for a particular vehicle.

The following assumptions are considered valid for the velocity–altitude range of the maneuver under investigation:

a) Parabolic-type vehicle drag polar

$$C_D = C_{D_0} + KC_L^2 \tag{7}$$

where C_{D_0} and K are assumed constant.

b) Exponential atmosphere

$$\rho = \rho_0 \exp(-\beta Z) \tag{8}$$

c) Constant gravitational acceleration $g = \text{const}$.

d) Flight-path angle bounded by the inequality $0 \leqq |\gamma| \leqq \pi/2$, which ensures that both the altitude and range are monotonic variables along any descent or ascent path. (See the Appendix for a discussion of the case $\gamma_D > \pi/2$).

e) Any maneuver is to be investigated by dividing it into a descent and ascent path, separated by the bottom point $\gamma = 0$ (This is a consequence of assumption a.)

The Allen and Eggers assumption that aerodynamic forces are dominant allows to rewrite the dynamic equations [Eqs. (3) and (4)] as

$$\dot{V} = -\rho SV^2C_D/2m \tag{9}$$

$$\dot{\gamma} = -\rho SVC_L/2m \tag{10}$$

Following Vinh,[10] one defines

1) The normalized lift coefficient

$$\lambda = C_L/C_L^* \tag{11}$$

where C_L^* is the lift coefficient at the maximum lift-to-drag ratio $E^* = C_L^*/C_D^* = 1/2(KC_{D_0})^{1/2}$.

2) The dimensionless independent variable

$$s = \int_0^t \beta V\,\mathrm{d}t \tag{12}$$

3) The dimensionless altitude, speed, range, and heat input variables

$$z = 2m\beta/SC_L^*\rho \tag{13}$$

$$v = \beta V^2/g \tag{14}$$

$$x = \beta X \tag{15}$$

$$q = 4\beta C_L^*Q/C_F'mg \tag{16}$$

Then, with the aid of the equation

$$\mathrm{d}\rho/\rho = -\beta\,\mathrm{d}Z \tag{17}$$

for the atmospheric density and

$$C_D = C_D^*(1+\lambda^2)/2 \tag{18}$$

for the drag coefficient and, using the dimensionless variables as defined above, the equations of motion (1), (2), (9), (10) and the heat-transfer equation (6) can be put into the dimensionless form

$$\mathrm{d}z/\mathrm{d}s = -z\sin\gamma \tag{19}$$

$$\mathrm{d}v/\mathrm{d}s = -(1+\lambda^2)v/E^*z \tag{20}$$

$$\mathrm{d}x/\mathrm{d}s = \cos\gamma \tag{21}$$

$$\mathrm{d}\gamma/\mathrm{d}s = -\lambda/z \tag{22}$$

$$\mathrm{d}q/\mathrm{d}s = 2zv \tag{23}$$

In this form, the equations are free of any physical parameters, except for E^* and the bound on the lift coefficient

$$|\lambda| \leqq \lambda_{\max} \tag{24}$$

where it was assumed for simplicity that $\lambda_{\min} = -\lambda_{\max}$

Analytical solutions for $\lambda = \text{const}$ can be conveniently obtained if the problem equations (19–23) are rewritten with respect to γ as an independent variable, integrated and combined to give

$$\cos\gamma = \lambda/z + C \tag{25}$$

$$v = v_i \exp[a(\gamma - \gamma_i)] \tag{26}$$

$$x = -\gamma - C\int_{\gamma_i}^{\gamma} \frac{\mathrm{d}\gamma}{\cos\gamma - C} + x_i + \gamma_i \tag{27}$$

$$t = t_i - \frac{\exp(a\gamma_i/2)}{\sqrt{\beta g v_i}} \int_{\gamma_i}^{\gamma} \frac{\exp(-a\gamma/2)}{\cos\gamma - C}\,\mathrm{d}\gamma \tag{28}$$

$$q = q_i - 2\lambda v_i \exp(-a\gamma_i) \int_{\gamma_i}^{\gamma} \frac{\exp(a\gamma)}{(\cos\gamma - C)^2}\,\mathrm{d}\gamma \tag{29}$$

where

$$C = \cos\gamma_i - (\lambda/z_i) \tag{30}$$

$$a = (1+\lambda^2)/\lambda E^* \tag{31}$$

The integral in the range equation (27) is given by[14]

$$\int \frac{\mathrm{d}\gamma}{\cos\gamma - C} = \frac{2}{\sqrt{C^2-1}} \tan^{-1} \frac{(C-1)\tan(\gamma/2)}{\sqrt{C^2-1}}, \qquad C > 1$$

$$= \tan(\gamma/2), \qquad C = 1$$

$$= \ell n \left| \frac{(1-C)\tan(\gamma/2) + \sqrt{1-C^2}}{(1-C)\tan(\gamma/2) - \sqrt{1-C^2}} \right|, \qquad C < 1 \tag{32}$$

while the integrals in Eqs. (28) and (29) can be computed by simple quadratures [note that reverting to the dimensional time t introduces the physical parameters β and g into solution (28)].

Formulation of the Problem and Region of Admissible Paths

As a first step, the problem equations (19–23) are rewritten with respect to z as an independent variable in the following form

$$d\gamma/dz = \lambda/z^2 \sin\gamma \tag{33}$$

$$dv/dz = (1+\lambda^2)\, v/E^* z^2 \sin\gamma \tag{34}$$

$$dx/dz = -1/z \tan\gamma \tag{35}$$

$$dt/dz = -1/\sqrt{g\beta v}\, z \sin\gamma \tag{36}$$

$$dq/dz = -2v/\sin\gamma \tag{37}$$

The problem is therefore described by five equations [Eqs. (33–37)] involving one independent variable (z) and six dependent variables ($\gamma, v, x, t, q, \lambda$), thus allowing use of the normalized lift coefficient λ as control variable. Consequently, for a given set of initial conditions, infinite trajectories exist that are physically and mathematically possible, more specifically, one trajectory for each arbitrarily prescribed lift modulation program $\lambda(z)$. However, the choice of this program is limited by the fact that the control is bounded by the following inequality, which must be satisfied at all points of the flight path

$$-\lambda_{max} \leqq \lambda \leqq \lambda_{max} \tag{38}$$

It can readily be seen that for any prescribed lift modulation program $\lambda(z)$ that does not violate Eq. (38), Eq. (33) yields by integration $\gamma(z)$, which can subsequently be used to obtain $v(z)$, $x(z)$, $t(z)$, and $q(z)$ by integrating Eqs. (34–37), respectively, the entire motion being thus known. Therefore, in a $z\gamma$ plane, the optimal lift control problem can be formulated as follows: In the class of functions $\gamma(z)$ that transfer a given vehicle from the initial state $I(z_I, \gamma_I)$ to the final state $F(z_F, \gamma_F)$ and are also consistent with Eq. (38), determine that particular function that extremizes a prescribed functional.

Under this formulation, the functionals which can be extremized are the nondimensional final velocity v, range x, time t, and heat input q.

Equations (25) and (30) can be used now for plotting the domain of admissible paths for a descent trajectory (Fig. 1). The two limiting lines $\lambda = \lambda_{max}$ and $\lambda = -\lambda_{max}$, beginning at point I, are obtained by calculating the integration constant C in terms of the known initial conditions, while the two limiting lines $\lambda = \lambda_{max}$ and $\lambda = -\lambda_{max}$ arriving at point F are analogously obtained in terms of the known final conditions. The contour IDFCI identified by these four limiting lines encloses the region of admissible paths, i.e., the region of the $z\gamma$ plane containing all the trajectories that are consistent with the prescribed end values of the altitude and flight-path angle. No trajectory connecting endpoints I and F may cross the boundary of this region without violating the inequality constraint, Eq. (38). Conversely, every trajectory internal to the admissible domain is physically possible provided that the lift coefficient constraint, Eq. (39), is satisfied.

Optimal Solutions by Green's Theorem

In a $z\gamma$-coordinate system, consider a linear functional, that is, a line integral that is linear in the derivative of the unknown function $\gamma(z)$

$$H = \int_I^F [\phi(z,\gamma) + \psi(z,\gamma)\gamma']\, dz \tag{39}$$

where $I(z_I, \gamma_I)$ and $F(z_F, \gamma_F)$ belong to the boundary of the admissible domain, where ϕ and ψ are known functions of z and γ, and where γ' denotes the derivative $d\gamma/dz$. If the two functions ϕ and ψ and their partial derivatives are continuous everywhere in an area bounded by two admissible paths IPF and IQF (descending, Fig. 2, or ascending, Fig. 3), then the relative advantage or disadvantage of one integration path with respect to another is given by the difference between the respective line integrals

$$\Delta H = \int_{IPF} (\phi dz + \psi d\gamma) - \int_{IQF} (\phi dz + \psi d\gamma)$$

$$= \oint_{IPFQI} (\phi dz + \psi d\gamma) \tag{40}$$

which may be transformed into a surface integral using Green's theorem

$$\oint_{IPFQI} (\phi dz + \psi d\gamma) = \iint_{(IPFQI)} \left(\frac{\partial \psi}{\partial z} - \frac{\partial \phi}{\partial \gamma} \right) dz\, d\gamma \tag{41}$$

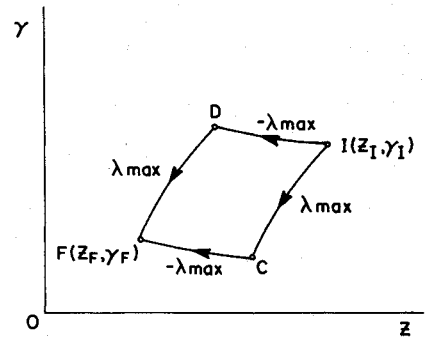

Fig. 1 Region of admissible arcs (descent paths).

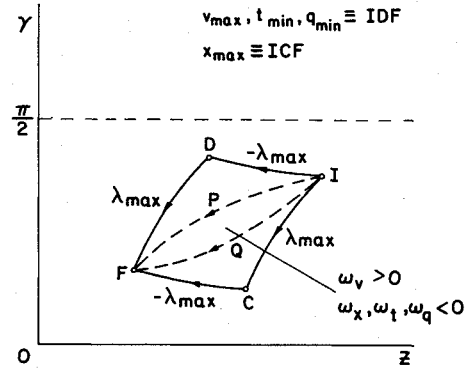

Fig. 2 Extremizing arcs for descent trajectories.

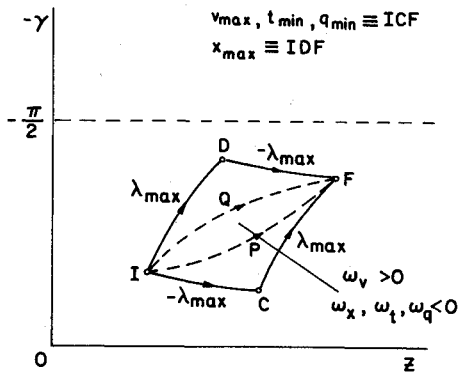

Fig. 3 Extremizing arcs for ascent trajectories.

and rewritten in the form

$$\Delta H = \int\int_{(\mathrm{IPFQI})} \omega(z,\gamma)\,\mathrm{d}z\,\mathrm{d}\gamma \tag{42}$$

where ω denotes the fundamental function

$$\omega(z,\gamma) = \frac{\partial\psi}{\partial z} - \frac{\partial\phi}{\partial\gamma} \tag{43}$$

The transformation of integrals is accompanied by a positive sign when proceeding counterclockwise along the integration path and by a negative sign when proceeding clockwise.

If the function ω has the same sign everywhere within the admissible domain (which will be shown to be the case in this analysis), three possibilities exist: ω is positive, negative, or zero. If the function is positive, Eq. (42) leads to

$$\Delta H > 0 \tag{44}$$

which implies that

$$H_{\mathrm{IPF}} > H_{\mathrm{IQF}} \tag{45}$$

By the same reasoning, any path to the right of IPF yields a further increase in the value of the integral, while any path to the left of IQF yields a further decrease in the value of the integral. Thus, by a limiting process, the following conclusions are reached for both descending or ascending trajectories (Figs. 2 and 3, respectively):

1) The integral (39) is *maximized* by either the path IDF (Fig. 2) or ICF (Fig. 3), both of which are located on the boundary of the admissible domains (−max lift/max lift) and are traveled in such a way that these domains are always on the left.

2) The integral [Eq. (39)] is *minimized* by either the path ICF (Fig. 2) or IDF (Fig. 3), both of which are located on the boundary of the admissible domains (max lift/− max lift) and are traveled in such a way that these domains are always on the right.

The results relative to the case where $\omega < 0$ are identical to those relative to the case where $\omega > 0$, except that maximum paths are transformed into minimum paths and vice versa. Finally, the case where $\omega = 0$ everywhere is degenerate in that the integral [Eq. (39)] becomes independent of the integration path.

Extremization of the Final Velocity

From Eq. (34) one has

$$\mathrm{d}v = \phi_v\,\mathrm{d}z \tag{46}$$

where

$$\phi_v(z,\gamma) = \frac{(1+\lambda^2)\,v(z)}{E^* z^2 \sin\gamma} \tag{47}$$

and $v(z)$ is a functional depending on the integration path $\gamma(z)$. Consequently, for a given initial velocity v_{I}, the linear functional to be extremized is given by

$$H_v = v_{\mathrm{F}} - v_{\mathrm{I}} = \int_{z_{\mathrm{I}}}^{z_{\mathrm{F}}} \phi_v\,\mathrm{d}z \tag{48}$$

and the fundamental function takes the form

$$\omega_v(z,\gamma) = -\frac{\partial\phi_v}{\partial\gamma} = \frac{(1+\lambda^2)\,v(z)\cos\gamma}{E^* z^2 \sin^2\gamma} \tag{49}$$

In view of assumption d, ω_v is positive everywhere within the admissible domain for ascent or decent paths; therefore, the final velocity is maximized by the path IDF (Fig. 2) or ICF (Fig. 3) and minimized by the path ICF (Fig. 2) or IDF (Fig. 3). The optimal maneuver yielding maximum final velocity is composed of a minimum-lift subarc, followed by a maximum-lift subarc (nonsingular subarcs in variational terminology). Similar conclusions have been obtained in Ref. 15 via a variational approach.

The analyses of the other payoffs being similar to the one above, the results are given below without details.

Extremization of the Range

From Eq. (35) the fundamental function is obtained as

$$\omega_x(z,\gamma) = -\frac{\partial\phi_x}{\partial\gamma} = -\frac{1}{z\sin^2\gamma} \tag{50}$$

and is negative everywhere within the admissible domains. Accordingly, the optimum maneuver yielding a maximum range is a maximum-lift subarc, followed by a minimum-lift subarc (ICF for descent, Fig. 2, and IDF for ascent, Fig. 3).

Extremization of the Time

The fundamental function is obtained from Eq. (36) as

$$\omega_t(z,\gamma) = -\frac{\partial\phi_t}{\partial\gamma} = -\frac{\cos\gamma}{\sqrt{g\beta v(z)}\,z\sin^2\gamma} \tag{51}$$

and is negative everywhere within the admissible domains. The optimal path yielding a minimum time transfer consists of a minimum-lift subarc, followed by a maximum-lift subarc (IDF for descent, Fig. 2, and ICF for ascent, Fig. 3).

Extremization of the Heat Input

Equation (37) yields the fundamental function as

$$\omega_q(z,\gamma) = -\frac{\partial\phi_q}{\partial\gamma} = -\frac{2v(z)\cos\gamma}{\sin^2\gamma} \tag{52}$$

which is negative everywhere within the admissible domains. The optimal maneuver leading to minimum heat input consists of a minimum-lift subarc, followed by a maximum-lift subarc (IDF for descent, Fig. 2, and ICF for ascent, Fig. 3).

It is important to note that the functions ϕ_v, ϕ_x, ϕ_t, and ϕ_q and their partial derivatives are discontinuous at $\gamma = 0$ (the bottom point of a skip trajectory). For this reason, the present analysis applies only to monotonically descending or ascending trajectories, as ensured by the inequality constraint of assumption d. This is geometrically equivalent to simple conex configurations of the admissible domain.

Existence Conditions for Max-Lift/Min-Lift and Min-Lift/Max-Lift Trajectories

The optimal lift control laws developed in the previous section are based on the implicit assumption that the vehicle can be transferred from the initial to the final state using only $\lambda_{\max}/-\lambda_{\max}$ or $-\lambda_{\max}/\lambda_{\max}$ trajectories. Conditions for this assumption to be valid are developed below.

Descent Trajectories ($z_{\mathrm{I}} > z_{\mathrm{F}}$, $\gamma > 0$, Fig. 2)

Min-Lift/Max-Lift Paths (IDF)

From Eqs. (25) and (30), the expression of $\gamma(z)$ along subarc ID($\lambda = -\lambda_{\max}$) is obtained as

$$\cos\gamma = -(\lambda_{\max}/z) + C_{\mathrm{ID}} \tag{53}$$

$$C_{\mathrm{ID}} = \cos\gamma_{\mathrm{I}} + (\lambda_{\max}/z_{\mathrm{I}}) \tag{54}$$

and along subarc DF($\lambda = \lambda_{max}$) as

$$\cos\gamma = (\lambda_{max}/z) + C_{DF} \quad (55)$$

$$C_{DF} = \cos\gamma_D - (\lambda_{max}/z_D) \quad (56)$$

The coordinates of the switching point D in the $z-\gamma$ plane are obtained by intersecting the ID and DF subarcs

$$z_D = 2\lambda_{max}\Big/\left[\cos\gamma_I - \cos\gamma_F + \lambda_{max}\left(\frac{1}{z_I} + \frac{1}{z_F}\right)\right] \quad (57)$$

$$\gamma_D = \arccos[-(\lambda_{max}/z_D) + C_{ID}] \quad (58)$$

The conditions for $F(z_F, \gamma_F)$ to be reachable from $I(z_I, \gamma_I)$ by a descending $-\lambda_{max}/\lambda_{max}$ trajectory are

$$z_F \leqq z_D \leqq z_I \quad (59)$$

$$\gamma_D \leqq \pi/2 \quad (60)$$

which results in the following set of inequality constraints

$$\cos\gamma_I - \cos\gamma_F + \lambda_{max}[(1/z_I) - (1/z_F)] < 0 \quad (61)$$

$$\cos\gamma_F - \cos\gamma_I + \lambda_{max}[(1/z_I) - (1/z_F)] < 0 \quad (62)$$

$$\cos\gamma_I + \cos\gamma_F + \lambda_{max}[(1/z_I) - (1/z_F)] > 0 \quad (63)$$

Inspection of the above inequalities shows that for any given set of data (z_I, γ_I, z_F, γ_F, and λ_{max}), one of the two conditions (61) and (62) is always satisfied (which one depends on whether $\gamma_I > \gamma_F$ or $\gamma_I < \gamma_F$). This leaves two inequalities to be used for drawing boundaries of domains of admissible z_F and γ_F values for prescribed values of z_I, γ_I, and λ_{max}, as shown in Fig. 4. Higher λ_{max} will broaden the domain for this type of path.

The analyses of the remaining types of paths proceed as indicated above, so that only the results are summarized in the following.

Max-Lift / Min-Lift Paths (ICF)

The conditions for $F(Z_F, \gamma_F)$ to be reachable from $I(z_I, \gamma_I)$ by a descending $\lambda_{max}/-\lambda_{max}$ trajectory (switching point C) are

$$z_F \leqq z_C \leqq z_I \quad (64)$$

$$\gamma_C \geqq 0 \quad (65)$$

leading to a set of constraints consisting of Eqs. (62), (63), and

$$\cos\gamma_I + \cos\gamma_F + \lambda_{max}[(1/z_F) - (1/z_I)] - 2 < 0 \quad (66)$$

A typical domain of admissible z_F and γ_F values is shown in Fig. 5, where it can be seen that the range of feasible z_F decreases as γ_F decreases and reduces to a single z_F value for $\gamma_F = 0$, when the trajectory becomes a positive lift arc (C ≡ F).

Ascent Trajectories ($z_I < z_F$, $\gamma < 0$, Fig. 3)

Note that subscripts I, F, C, and D used here refer to *ascent* trajectories and denote quantities different from those related to the *descent* trajectories of the previous subsection.

Max-Lift / Min-Lift Paths (IDF)

The conditions for $F(z_F, \gamma_F)$ to be reachable from $I(z_I, \gamma_I)$ by an ascending $\lambda_{max}/-\lambda_{max}$ trajectory (switching point D) are Eq. (60) and

$$z_I \leqq z_D \leqq z_F \quad (67)$$

yielding the following set of inequality constraints

$$\cos\gamma_F - \cos\gamma_I + \lambda_{max}[(1/z_I) - (1/z_F)] > 0 \quad (68)$$

$$\cos\gamma_I - \cos\gamma_F + \lambda_{max}[(1/z_I) - (1/z_F)] > 0 \quad (69)$$

$$\cos\gamma_I + \cos\gamma_F + \lambda_{max}[(1/z_F) - (1/z_I)] > 0 \quad (70)$$

Figure 6 illustrates the domain of admissible z_F and γ_F values, which for the particular set of z_I, γ_I, and λ_{max} values chosen is seen to be bounded only on the lower z_F side. Higher λ_{max} will increase the range of feasible z_F values.

Min-Lift / Max-Lift Paths (ICF)

The conditions for $F(z_F, \gamma_F)$ to be reachable from $I(z_I, \gamma_I)$ by an ascending $-\lambda_{max}/\lambda_{max}$ trajectory (switching point C)

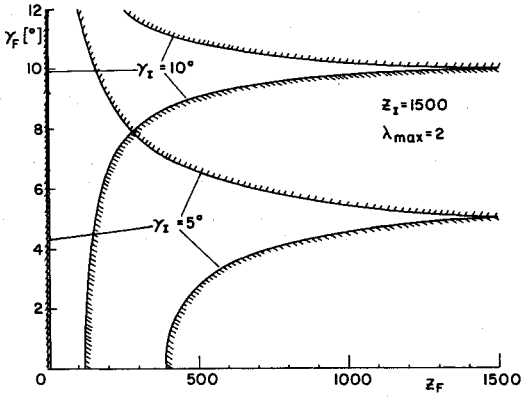

Fig. 4 Domain of admissible final altitudes and flight-path angles for − max-lift / max-lift descent trajectories.

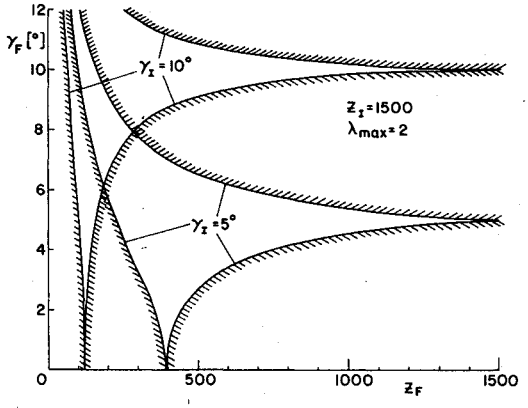

Fig. 5 Domain of admissible final altitudes and flight-path angles for max-lift / − max-lift descent trajectories.

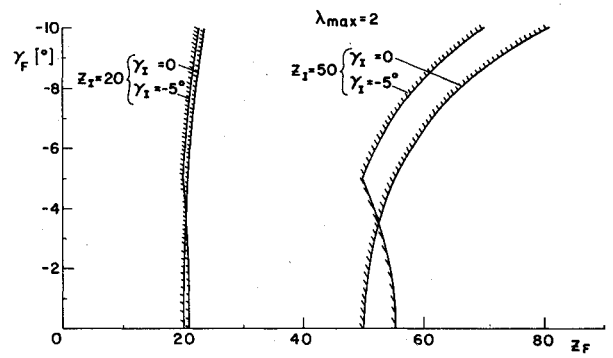

Fig. 6 Domain of admissible final altitudes and flight-path angles for max-lift / − max-lift ascent trajectories.

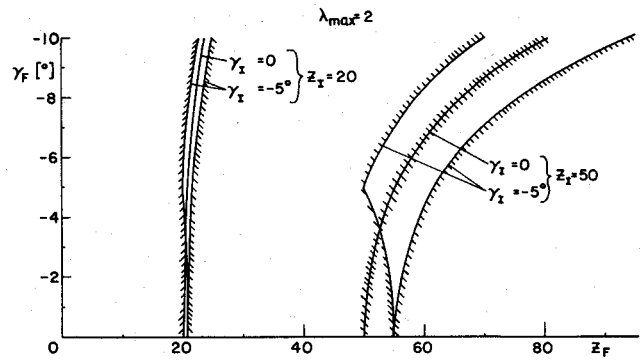

Fig. 7 Domain of admissible final altitudes and flight-path angles for −max-lift/max-lift ascent trajectories.

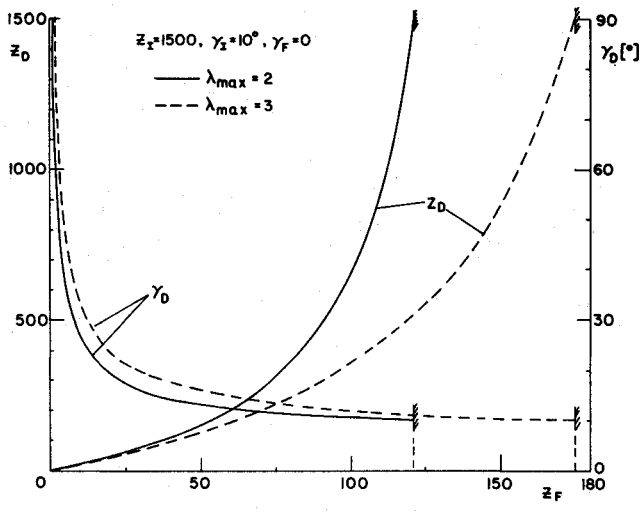

Fig. 8 Altitude and flight-path angle of switching points for −max-lift /max-lift descent trajectories.

are Eq. (65) and

$$z_I \leqq z_C \leqq z_F \tag{71}$$

leading to a set of constraints consisting of Eqs. (69), (68), and

$$\cos\gamma_I + \cos\gamma_F + \lambda_{max}[(1/z_I) - (1/z_F)] - 2 < 0 \tag{72}$$

A domain of admissible z_F and γ_F values is plotted in Fig. 7, where it can be remarked that the range of admissible z_F narrows for lower z_I and $|\gamma_I|$ and reduces to a single z_F value for $\gamma_I = 0$, when the trajectory becomes a positive lift arc (C ≡ I).

Switching Points

The altitude and flight-path angle of switching points on any feasible trajectory can be computed using Eqs. (57–58) and similar ones that can be easily derived for the other types of paths considered above. As an illustration, Fig. 8 shows that for a descending $-\lambda_{max}/\lambda_{max}$ path, the switching point occurs at lower altitudes for higher maximum lift. On the other hand, for fixed λ_{max}, the switching point moves upward as z_F decreases and, for the lowest feasible z_F, the switching point reaches the initial point. Figure 9 shows that the switching altitude z_C decreases with higher γ_I and lower λ_{max} for descent paths,with $\gamma_F = 0$. As already pointed out in Fig. 5, z_C coincides in this case with z_F, and the whole trajectory is flown with maximum lift.

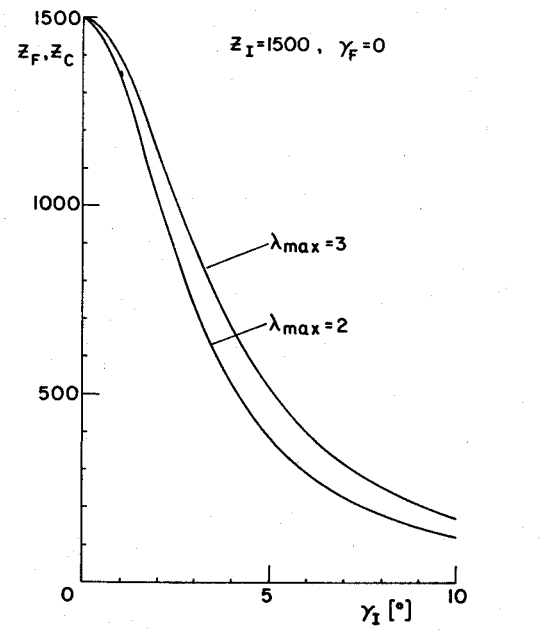

Fig. 9 Admissible final altitudes for max-lift descent trajectories with zero final flight-path angle.

Numerical Results

A parametric study has been conducted in order to get some insight into the influence of various parameters on the four payoffs, namely, final velocity, range, time, and heat input. For the sake of brevity, only descent trajectories are considered. The relationships given below are obtained from Eqs. (25–31) and (53–58), with all angle values in radians.

1) Min-lift/max-lift descent path (IDF)

− maximum final velocity (v_I given)

$$v_F = v_D \exp[a_{DF}(\gamma_F - \gamma_D)] \tag{73}$$

where

$$v_D = v_I \exp[a_{ID}(\gamma_D - \gamma_I)] \tag{74}$$

$$a_{ID} = -(1 + \lambda_{max}^2)/\lambda_{max} E^* \tag{75}$$

$$a_{DF} = (1 + \lambda_{max}^2)/\lambda_{max} E^* \tag{76}$$

− minimum time

$$t_{IF} = t_{ID} - \frac{\exp(a_{DF}\gamma_D/2)}{\sqrt{\beta g v_D}} \int_{\gamma_D}^{\gamma_F} \frac{\exp(-a_{DF}\gamma/2)}{\cos\gamma - C_{DF}} d\gamma \tag{77}$$

where

$$t_{ID} = -\frac{\exp(a_{ID}\gamma_I/2)}{\sqrt{\beta g v_I}} \int_{\gamma_I}^{\gamma_D} \frac{\exp(-a_{ID}\gamma/2)}{\cos\gamma - C_{ID}} d\gamma \tag{78}$$

− minimum heat input

$$q_{IF} = q_{ID} - 2\lambda_{max} v_D \exp(-a_{DF}\gamma_D) \int_{\gamma_D}^{\gamma_F} \frac{\exp(a_{DF}\gamma)}{(\cos\gamma - C_{DF})^2} d\gamma \tag{79}$$

where

$$q_{ID} = 2\lambda_{max} V_I \exp(-a_{ID}\gamma_I) \int_{\gamma_I}^{\gamma_D} \left[\frac{\exp(a_{ID}\gamma)}{(\cos\gamma - C_{ID})^2}\right] d\gamma \tag{80}$$

2) Max-lift/min-lift descent path (ICF)
– maximum range

$$x_{IF} = x_{IC} - \gamma_F + \gamma_c$$

$$-\frac{2C_{CF}}{\sqrt{C_{CF}^2-1}}\tan^{-1}\frac{\sqrt{C_{CF}^2-1}\tan(\gamma/2)}{1-C_{CF}}\Bigg|_{\gamma_c}^{\gamma_F} \qquad (81)$$

for $C_{CF} > 1$, and

$$x_{IF} = x_{IC} - \gamma_F + \gamma_c$$

$$-\frac{C_{CF}}{\sqrt{1-C_{CF}^2}}\ell n\left|\frac{\sqrt{1-C_{CF}^2}\tan(\gamma/2)+1-C_{CF}}{\sqrt{1-C_{CF}^2}\tan(\gamma/2)-1+C_{CF}}\right|\Bigg|_{\gamma_c}^{\gamma_F} \qquad (82)$$

for $C_{CF} < 1$, where

$$x_{IC} = -\gamma_c + \gamma_I$$

$$-\frac{C_{IC}}{\sqrt{1-C_{IC}^2}}\ell n\left|\frac{\sqrt{1-C_{IC}^2}\tan(\gamma/2)+1-C_{IC}}{\sqrt{1-C_{IC}^2}\tan(\gamma/2)-1+C_{IC}}\right|\Bigg|_{\gamma_I}^{\gamma_c} \qquad (83)$$

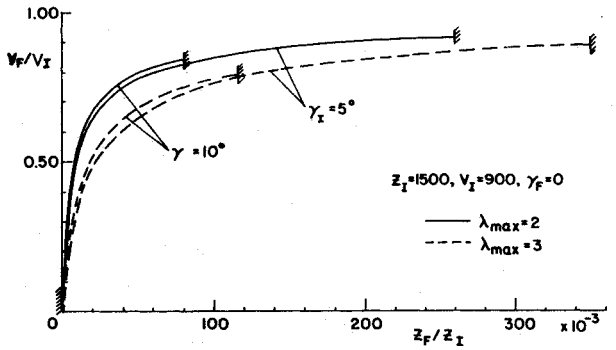

Fig. 10 Maximum final velocity vs final altitude for descent paths with horizontal terminal flight.

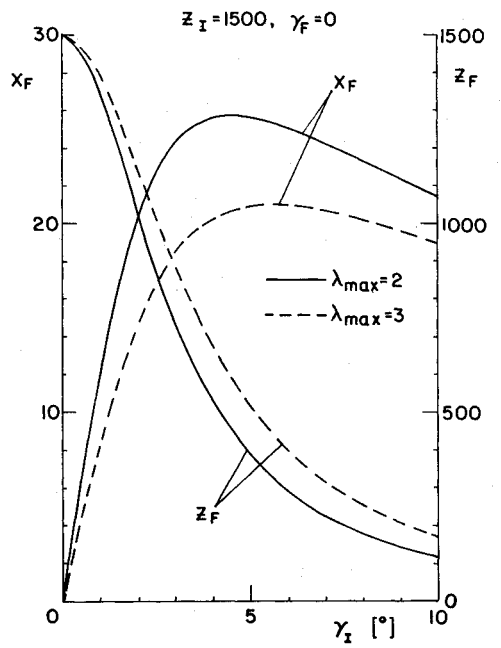

Fig. 11 Maximum range vs entry angle and final altitude for descent paths with horizontal terminal flight.

$$C_{IC} = \cos\gamma_I - (\lambda_{max}/z_I) \qquad (C_{IC} < 1) \qquad (84)$$

$$C_{CF} = \cos\gamma_C + (\lambda_{max}/z_C) \qquad (85)$$

The results are presented in Figs. 10–13 for the optimal velocity, range, time, and heat input, respectively. All the trajectories investigated start from $z_I = 1500$ and must reach horizontal position $\gamma_F = 0$ at various z_F, for $\gamma_I = 5$ or 10 deg and $\lambda_{max} = 2$ or 3. The payoffs being in nondimensional form (except for the time), the graphs permit rapid performance estimations and comparative analyses of various maneuvers. If different parameter values are desired, the closed-form solutions [Eqs. (73–85)] can be used with a minimum of computational effort. An inspection of the graphs shows that—everything else being equal—steeper entry angles yield higher final

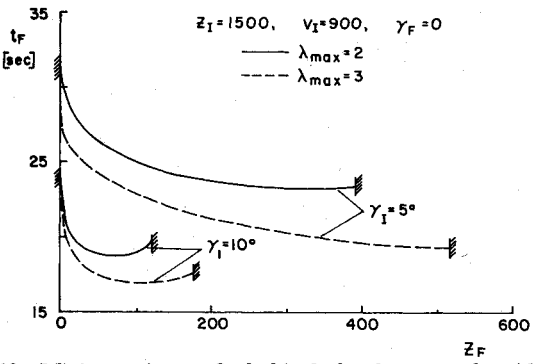

Fig. 12 Minimum time vs final altitude for descent paths with horizontal terminal flight.

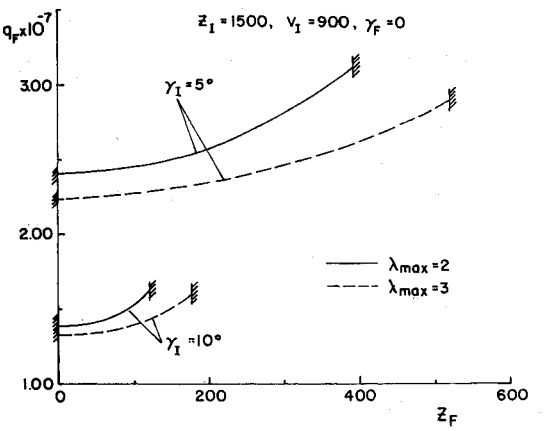

Fig. 13 Minimum heat input vs final altitude for descent paths with horizontal terminal flight.

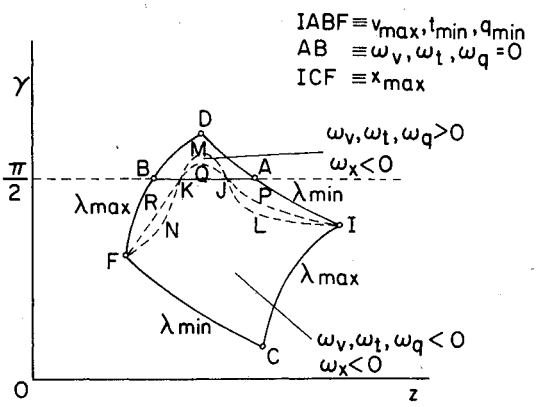

Fig. 14 Extremizing arcs for descent trajectories with $\gamma_D > \pi/2$.

velocities, shorter flight durations, and lower heat inputs. On the other hand, higher maximum lift yields lower final velocities, shorter flight durations, lower heat inputs, and shorter ranges. Higher final altitudes yield higher final velocities, lower flight durations, and heat inputs, but only for smaller entry angles. For higher entry angles, there appears to be a z_F value yielding a minimum-minimorum t_F and q_F value, and the same is true of a $\gamma_I - z_F$ combination yielding a maximum-maximorum x_F value.

Summary and Conclusions

A method allowing a rapid estimation of optimal re-entry maneuvers in the vertical plane is presented for the case in which the maximum lift coefficient is bounded. It is assumed that the trajectory involves only maximum positive and/or negative lift subarcs, and conditions for the existence of such trajectories are derived. The approach shows how to control the lift in order to transfer the vehicle between prescribed initial and final altitudes and flight-path angles, while extremizing either the final velocity, the range, the flight duration, or the heat input. The maneuver under consideration must be divided into descending or ascending subarcs which are analyzed separately. Closed-form solutions for velocity, range, time, and heat input are derived, along with formulas for determining the switching points. It is shown that: 1) a min-lift/max-lift maneuver maximizes the final velocity and minimizes the time and the heat input; 2) a max-lift/min-lift maneuver maximizes the range. Results of parametric studies are presented in graphical nondimensional form, allowing rapid comparative analyses of different maneuvers. For optimal descending trajectories ending in a horizontal position, it is shown that: 1) higher entry angles yield higher final velocities and lower flight durations and heat inputs; 2) higher maximum lift yields lower final velocities, flight durations and heat inputs, and shorter ranges.

Appendix: Singular Vertical Subarcs

If point D lies above the $\gamma = \pi/2$ line, the sign of fundamental functions ω_v, ω_t, and ω_q is no longer constant within the admissible domain. The line $\gamma = \pi/2$ represents the locus of the points where these functions vanish, intersecting the boundary of the admissible domain at A and B. Figure 14 shows the signs of ω_v, ω_t, and ω_q, as resulting from Eqs. (59), (51), and (52).

Consider now two admissible paths IPJQKRF and ILJMKNF, which intersect the line $\omega_v = 0$ at two arbitrarily specified points J and K. The difference between the line integrals for these paths is given by

$$\Delta H_v = \int_{\text{IPJQKRF}} \phi_v \, dz - \int_{\text{ILJMKNF}} \phi_v \, dz \tag{A1}$$

and can be rewritten as

$$\Delta H_v = \int_{\text{IPJLI}} \phi_v \, dz + \int_{\text{JQKMJ}} \phi_v \, dz + \int_{\text{KRFNK}} \phi_v \, dz \tag{A2}$$

Remarking that circuits IPJLI and KRFNK are traveled counterclockwise, while circuit JQKMJ is traveled clockwise, application of Green's theorem yields

$$\Delta H_v = \iint_{(\text{IPJLI})} \omega_v \, dz \, d\gamma - \iint_{(\text{JQKMJ})} \omega_v \, dz \, d\gamma + \iint_{(\text{KRFNK})} \omega_v \, dz \, d\gamma \tag{A3}$$

Since ω_v is positive within the areas (IPJLI) and (KRFNK), being negative within the area (JQKMJ), ΔH_v is positive, which implies that

$$H_{v_{\text{IPJQKRF}}} > H_{v_{\text{ILJMKNF}}} \tag{A4}$$

Therefore, any path that is closer to the line $\omega_v = 0$ than the path IPJQKRF will increase the value of H_v. By a limiting process, the path IABF can be shown to yield the highest value of the integral in the class of arcs that pass through the prescribed endpoints and intersect the line $\omega_v = 0$ at two arbitrarily specified points J and K.

The final step is to compare the path IABF with another crossing the line $\omega_v = 0$ at an arbitrary number of points or not crossing this line. It can be shown by further application of Green's theorem that the path IABF maximizes the linear integral (48) with respect to every possible admissible path. Hence, if the flight-path angle reaches a value of $\pi/2$ at a certain point on the minimum-lift subarc ID, then the optimum path that maximizes the final velocity is a minimum-lift subarc IA until $\gamma = \pi/2$, followed by a vertical subarc AB (singular arc in variational terminology), and finally a maximum-lift subarc BF reaching the final point.[15] By a similar reasoning, it can be shown that the path IABF also minimizes the time and the heat input. The lift control, velocity, time, and heat input along the vertical singular subarc AB are obtained with $\gamma = \pi/2$ from Eqs. (33–34) and (36–37) as follows:

$$\lambda = 0 \tag{A5}$$

$$v = v_A \exp(1/E^* z_A) \exp(-1/E^* z) \tag{A6}$$

$$t - t_A = \frac{\exp(-1/2E^* z_A)}{\sqrt{g\beta v_A}} \left[Ei\left(\frac{1}{2E^* z}\right) - Ei\left(\frac{1}{2E^* z_A}\right) \right] \tag{A7}$$

$$q - q_A = -\frac{2v_A}{E^*} \exp\left(\frac{1}{E^* z_A}\right) \times \left[E^* z \exp\left(-\frac{1}{E^* z}\right) + Ei\left(-\frac{1}{E^* z}\right) \right]_{z_A}^{z} \tag{A8}$$

References

[1]Allen, H.J. and Eggers, A.J. Jr., "A Study of Motion and Aerodynamic Heating of Missiles Entering the Earth's Atmosphere at High Supersonic Speeds," NACA Rept. 1381, 1958.

[2]Contensou, P., "Contribution a l'Étude Schématique des Trajectoires Semiballistiques à Grande Portée," Communication Presented to ATMA, Paris, 1965.

[3]Busemann, A., Vinh, N.X., and Kelley, G., "Optimum Maneuvers of Hypervelocity Vehicles," NASA CR-1078, 1968.

[4]Busemann, A., Vinh, N.X., and Kelley, G., "Optimum Maneuvers of a Skip Vehicle with Bounded Lift Constraints," *Journal of Optimization Theory and Applications*, Vol. 3, No. 4, 1969, pp. 243–262.

[5]Dickmanns, E.D., "Optimal Control for Synergetic Plane Change," *Proceedings of the XXth International Astronautical Congress, Mar del Plata, Argentina, 1969*, edited by G. Lunc, Pergamon Press, Oxford, England, 1972, pp. 597–631.

[6]Speyer, J.L. and Womble, M.E., "Approximate Optimal Atmospheric Entry Trajectories," *Journal of Spacecraft and Rockets*, Vol. 8, Nov. 1971, pp. 1120–1125.

[7]Griffin, J.W. Jr. and Vinh, N.X., "Three-Dimensional Optimal Maneuvers of Hypervelocity Vehicles,"AIAA Paper 71-920.

[8]Beiner, L., "Maximum Aerodynamical Orbit Plane Change with Given Energy Loss by a Three-Dimensional Altitude—Constrained Skip Maneuver," *Zeitschrift für Flugwissenschaften*, Vol. 24, 1976, pp. 288–291.

[9]Beiner, L., "Optimal Three-Dimensional Aerodynamic Maneuver for a Shuttle Vehicle," *Israel Journal of Technology*, Vol. 16, 1978, pp. 45–55.

[10]Vinh, N.X., *Optimal Trajectories in Atmospheric Flight*, Elsevier, Amsterdam, 1981.

[11]Miele, A., "Extremization of Linear Integrals by Green's Theorem," *Optimization Techniques with Applications to Aerospace Systems*, edited by G. Leitmann, Academic Press, New York, 1962.

[12]Beiner, L., "Optimal Lift Control by Miele's Method for the Atmospheric Entry of a Hypersonic Glider: I. Simple Type Problems," *Revue Roumaine des Sciences Techniques–Mécanique Appliquée*, Vol. 17, No. 4, 1972, pp. 745–755.

[13]Loh, W.H.T., *Re-entry and Planetary Entry: Physics and Technology*, Vol. 1, Speringer-Verlag, New York, 1968, Ch. 2.

[14]Gradstein, I.S. and Ryzhik, I.M., *Tables of Integrals, Sums, Series and Products*, Nauka, Moscow, 1971 (in Russian).

[15]Shi, Y.Y., Pottsepp, L., and Eckstein, M.C., "Optimal Lift Control of a Hypersonic Lifting Body During Atmospheric Entry," *AIAA Journal*, Vol. 7, Dec. 1969, pp. 2233–2240.